Materials Science in Semiconductor Processing 144 (2022) 106570

Contents lists available at ScienceDirect

Materials Science in Semiconductor Processing

journal homepage: www.elsevier.com/locate/mssp

Sensitivity of polarized laser scattering detection to subsurface damage in ground silicon wafers

Jingfei Yin [a], Qian Bai [b], Bi Zhang [c,*]

[a] College of Mechanical and Electrical Engineering, Nanjing University of Aeronautics and Astronautics, Nanjing, 210016, China
[b] School of Mechanical Engineering, Dalian University of Technology, Dalian, 116024, China
[c] Department of Mechanical and Energy Engineering, Southern University of Science and Technology, Shenzhen, 518055, China

ARTICLE INFO

Keywords:
Subsurface damage
Polarized laser scattering
Silicon wafer
Grinding
Sensitivity

ABSTRACT

Silicon is the primary substrate material in the semiconductor industry. Since surface integrity of a silicon wafer is crucial to the performance of an IC chip made of the wafer, the subsurface damage (SSD) induced by machining to a silicon wafer has been intensively investigated. However, detecting SSD is a challenge due to a lack of an effective method. This study presents a novel method, the polarized laser scattering (PLS) method, for detecting SSD in ground silicon wafers. A PLS system is established to detect the grinding-induced SSD which is also evaluated by the destructive methods. The study shows that the PLS signal is sensitive to the SSD depth with a detection resolution of approximately 0.1 μm. In addition, the detectability of the PLS method is demonstrated and a relationship between the PLS signal and SSD depth is established to facilitate the practical applications of the PLS method.

1. Introduction

Wearable and portable electronic devices, such as smart phones, watches, and medical diagnostic devices, play important roles in our current life. They greatly improve our work efficiency and life quality. Most sensors and chips in the devices are manufactured based on a silicon wafer which is the primary substrate material in the semiconductor industry [1,2]. To meet the requirements of the devices, a silicon wafer has to be thinned from several hundred microns to a few tens of microns in thickness [3,4]. Generally, the thinning process of a silicon wafer is realized by precision back grinding. However, the silicon wafer is hard and brittle, it is easy to induce subsurface damage (SSD), known as cracks [5–7], dislocations [8], amorphous layer [9], etc. in a ground surface during grinding. Nowadays, the elevated performance of the electronic devices pushes the machining accuracy close to nanometric even atomic level, which requires extremely high surface integrity of the wafer. SSD degrades the surface integrity of a wafer and correspondingly is detrimental to the performance of a device made of the wafer. Therefore, it is crucial to reduce and remove the grinding-induced SSD. Detecting SSD can provide a guide to optimizing the grinding process, which is of significance to improve the surface integrity of the silicon wafer by grinding.

Methods for detecting SSD in a silicon wafer are divided into two types, namely, destructive and non-destructive, as reviewed by Yin et al. [10]. The processes of the destructive methods are relatively reliable. Moreover, destructive methods, such as the polishing method [11], fracture method [12], transmission electron microscopy (TEM) [13], etc., provide considerable detection accuracy and are thus still widely used. However, these methods impose clear limitations in low detection efficiency and destroying wafer. Therefore, Yin et al. [10]suggested that the non-destructive methods should be further studied and developed for SSD detection.

Many non-destructive methods have been developed to detecting SSD. Scanning acoustic microscopy (SAM) is widely applied to detecting the subsurface defects, such as voids, cracks, in the semiconductor industry [14]. The detection resolution of SAM is determined by the acoustic frequency. Higher frequency provides higher resolution. However, the acoustic attenuation of coupling increases with the frequency squared [15], which causes a decrease in penetration depth at an increased frequency. Generally, the frequency used in SAM is 10–400 MHz [16]. The resolution of a commercial SAM is about several microns which are not enough for detecting SSD in the ground wafers. The detection resolution of the acoustic methods can be improved by integrating other methods. Karabutov and Podymova [17] used the

* Corresponding author.
E-mail address: zhangb@sustech.edu.cn (B. Zhang).

https://doi.org/10.1016/j.mssp.2022.106570
Received 9 September 2021; Received in revised form 29 December 2021; Accepted 12 February 2022
Available online 23 February 2022

laser-ultrasonic method to detect the SSD depth in a machined silicon wafer and achieved the minimal reliably detectable depth of 0.15–0.2 μm. Ma and Arnold [14] claimed that the ultrasonic-based atomic force microscopy could extend the detection to subsurface defects in the nanoscale. Hardin et al. [18] found that the influence of the surface damage to the detection by an acoustic method was notable. Therefore, the influence of the surface damage on a ground silicon wafer cannot be avoided, which impedes the identification and quantification of SSD.

Cloetens et al. [19] used X-ray radiography and tomography to observe the subsurface damage in silicon. The micro cracks in silicon were clearly observed. However, X-ray radiation risks the operator's health. Moreover, the high-resolution imaging requires a small sample size limited to 1 mm in the three dimensions. Therefore, the high-resolution imaging via X-ray radiography and tomography is inapplicable to the detection of SSD in a ground wafer.

There are some methods for detecting residual stress in a ground silicon wafer, e.g., X-ray diffraction [20], Raman spectroscopy [21], and photoelastic method [22]. Residual stress is the result of SSD rather than an individual damage. If SSD is removed, residual stress is correspondingly relieved. The explicitly quantitative relations between the residual stress and SSD depth are too complicated to resolve. Therefore, these methods for detecting residual stress cannot detect the SSD depth in ground silicon wafers, which is, however, crucial to optimizing the grinding process.

Optical methods, such as optical coherence microscopy [23] and conventional confocal microscopy [24], are used to characterize SSD in ground glasses. The resolution of these optical methods is dependent on the used light wavelength. A shorter wavelength provides a higher resolution. The wavelength used in these methods is generally within the range of 300–700 nm which is fine for detecting the SSD in the transparent glasses. However, the penetration depth of the light in the range is considerably small for a silicon wafer [25]. Besides, a rough surface, e.g., a coarse-abrasive grinding surface, obstructs the detection of SSD [26]. Therefore, it is hard to see the optical coherence microscopy or conventional confocal microscopy applied to detecting SSD in silicon wafers.

Liao et al. [27] established a total internal reflection microscopy (TIRM) system to detect the SSD in optical components. TIRM is easy to conduct. However, it has a high requirement on the surface finish. A rough surface disturbs the detection of SSD [10]. Lu et al. [28] developed the cross-polarization confocal microscopy to detect the grinding-induced SSD in silicon wafers and obtained the quantitative evaluation of the SSD depth. The cross-polarization confocal microscopy integrates the polarized laser scattering (PLS) and confocal microscopy. Through this method, the influence of surface damage is greatly minimized. However, in Lu et al.'s study, only the laser scattering by the subsurface cracks was considered, the influence of other factors on the detection was neglected.

Yin et al. [29] considered residual stress-induced photoelasticity and proposed that the influence of the residual stress in a ground wafer could be minimized by aligning the polarization direction of the incident laser beam with the grinding marks in detecting SSD via the PLS method. Based on the proposition, Yin et al. [30] further achieved two-dimensional detection of SSD in the ground wafers by the PLS methods. They found that the SSD depth was the main factor in the PLS detection. However, the detection was only carried on the roughly ground wafer surface. As stated by Pei and Strasbaugh [31], fine grinding is important to reducing the SSD depth. The performance of the PLS detection on a finely ground wafer is unknown. In addition, an explicit model of the SSD depth was not provided, which obstructs the application of the PLS detection.

To reveal the performance and detectability of the PLS detection on the fine-ground wafers, this study uses the installed PLS system to detect the SSD in the wafers subjected to both course-grinding and fine-grinding processes. The sensitivity of the PLS detection to the SSD depth is studied. A relationship between the PLS signal and the SSD depth is attempted to build, which is important to expanding the application of the PLS method.

2. Experiments

The wafers used in this study were 200 mm in diameter and 575 μm in thickness with a polished (100) plane. The wafers were ground by an ultra-precision grinder (VG401 MKII, Okamoto, Japan), as shown in Fig. 1. Five wheels with different abrasive grit sizes were used for grinding the wafers. The grinding parameters are listed in Table 1. All the wafers were thinned by 50 μm in thickness. The spark-out grinding process has been commonly used to produce a wafer with the same SSD depth but lower surface roughness compared with the wafers without spark-out grinding. It is the process that the grinding wheel stops feeding but hangs over the workpiece surface until the grinding sparks vanish. When entering the spark-out process, the grinding system begins springing back. The grinding wheel gradually leaves the workpiece surface. Generally, spark-out grinding removes some high asperities on the ground surface. The depth of cut and amount of material removal in this process is far less than that in the conventional grinding process, therefore, the grinding force is considerably small. It turns out that the spark-out grinding hardly changes the SSD depth but reduces surface roughness.

The grinding-induced SSD in the wafers was detected by both the destructive methods and the PLS method. The destructive methods included the fracture method and TEM, the detail of the methods can be found in our previous paper [10]. The PLS detection was achieved by the self-installed PLS system, as shown in Fig. 2. The working principle of the PLS system is illustrated as follows. A laser beam was launched and then s-polarized after through a polarized beam splitter (PBS) with an extinction of 1,000. The s-polarized laser beam went through another PBS with an extinction of 3,000 and was then reflected to the object wafer by a reflector, as shown in Fig. (b). The lens used in the PLS system was to focus the laser beam to improve the detection resolution. The incident laser beam was scattered by SSD in the wafer. A part of the laser light was depolarized after scattering and then backscattered. The backscattered light was reflected to PBS by the reflector. The light with different polarization directions was split by PBS. A part of the backscattered light reserved the s-polarization that went through PBS, while the other part of the light with altered polarization, namely p-polarization, was reflected by PBS. The p-polarization light was then detected by a detector, as shown in Fig. 1(c). The Glan polarizer in front of the detector ensured that the light received by the detector was pure p-polarization. The intensity of the p-polarization was determined by SSD in the ground wafers. Therefore, the information of SSD was resolved based on the detected signal.

It has to be mentioned that the backscattered light from the wafer includes both the surface scattering light and the SSD-scattered light. The surface scattering can be regarded as a simple reflection by micro facets on the surface. Simple reflection does not alter the polarization of the scattered light, but multi-scattering does. If the surface roughness is small enough, the multi-scattering on the surface can be neglected. In this case, the surface-scattered light preserves the same polarization as the incident light [32]. Due to the complicated microstructure of SSD, the light is multi-scattered by SSD, which alters the polarization of the SSD-scattered light. Since the scattering light and the SSD-scattered light are in different polarization, they can be split, correspondingly, SSD can be detected and evaluated by the PLS method.

The study used a continuous-wave laser (MLL–III–914, CNI, China) with a wavelength of 914 nm. Based on the optical properties of the silicon wafer [25], the penetration depth of the laser beam was about 200 μm which was large enough to cover the SSD depth in this study. The output laser power was 15 mW. The detector was a silicon-based PIN diode (S3072, Hamamatsu, Japan). The minimum detectable light power of the detector was −41 dBm (80 nW). The maximum subsurface damage depth that could be measured in this study was about 200 μm.

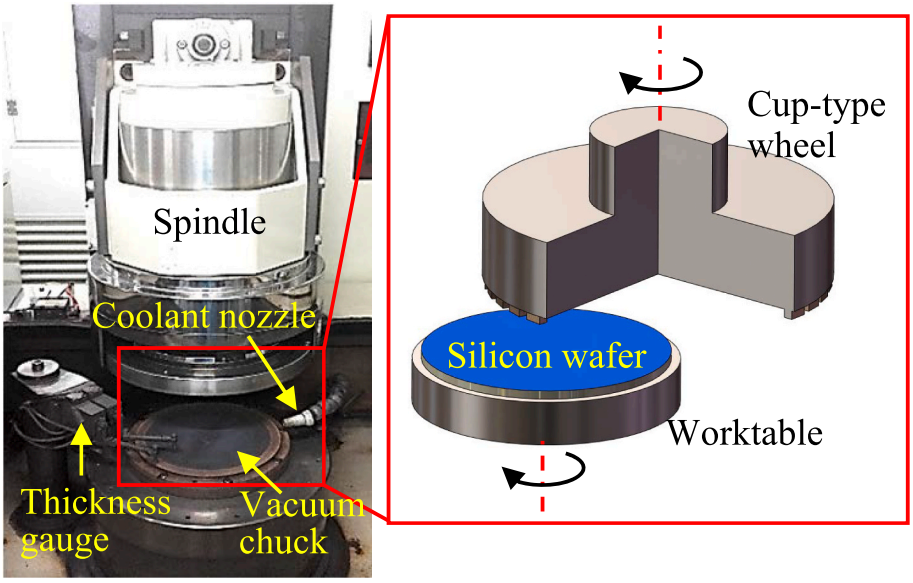

Fig. 1. Photographic view of the grinder and the schematic diagram of grinding arrangement.

Table 1
Grinding parameters used in the study.

Grinding parameters	Values
Wheel rotation speed, rpm	2,399
Worktable rotation speed, rpm	120
Feed rate, μm/min	90, 20, 10, 3
Mesh number of the wheels	#400, #600, #3,000, #5,000, #20,000
Spark-out duration, s	0, 10
Coolant	Deionized water

The focal length of the lens was about 5 mm. In the PLS detection, the distance of the lens to the wafer surface was set as 5 mm, the spot size on the wafer surface was approximately 10 μm.

Before the PLS detection, the study verified the influence of the surface roughness and SSD depth, in case the roughly ground surface leads to the depolarization of the surface scattering [32]. The wafer samples were carefully selected and prepared. The samples with the same surface roughness but different SSD depths were used to verify the influence of SSD depth. The samples with the same SSD depth but different surface roughness were used to verify the influence of surface roughness. And then, the ground wafers and one polished wafer were used for SSD detection by the PLS system. During the PLS detection, the polarization direction of the incident laser beam was aligned to the grinding marks. The detected PLS signals of the ground wafers were normalized by that of the polished wafer. By comparing the detected signals with the SSD depth, a relationship between the signal and SSD depth was built.

3. Results

The larger abrasive size engaged in grinding, the larger depth of cut produced the abrasives, which is common in grinding hard and brittle materials. The main damage type in the wafers ground by the #400 and #600 wheels is subsurface crack, as shown in Fig. 3 (a). When the mesh number of the abrasive in the wheel was larger than #3,000, the subsurface was crack-free. The predominant damage types were dislocations and amorphization, as shown in Fig. 3(b)–(d), which is also reported in other places [31,33]. The SSD depth distributions in the ground wafers are shown in Fig. 4. The SSD depths in the wafers ground by the #400 and #600 wheels were approximately 10 μm and 5 μm, respectively. While the SSD depths in the wafers ground by the #3,000 wheel, the #5,000 wheel, and the #20,000 wheel are lower than 1 μm. Therefore, the scattering sources of PLS detection are different in detecting the SSD of those ground wafers. For the wafers ground by #400 and #600 wheels, the PLS signal results from the scattering by both cracks and disordered crystal lattice. While for the rest wafers, the PLS signal is mainly caused by the disordered crystal lattice rather than cracks.

The verifications of the influence of surface roughness and SSD depth are illustrated as follows. Figs. 5 and 6 show surface and subsurface morphologies of the chosen wafer samples. Fig. 7 represents the

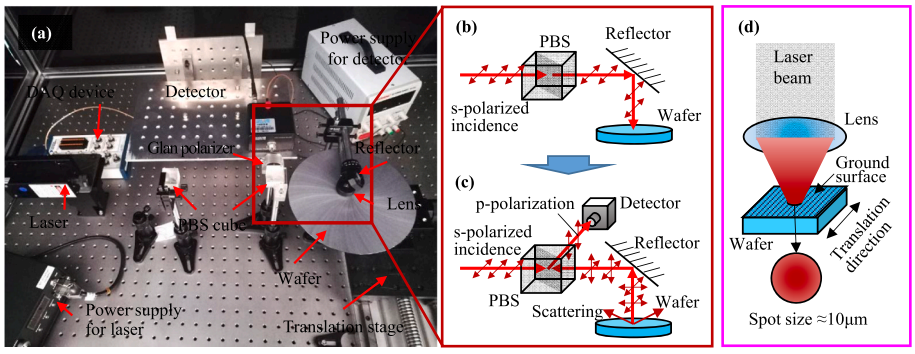

Fig. 2. The PLS system used in this study. (a) photographic picture of the PLS system, (b) schematics of the incident light path, (c) schematics of the backscattering light path, (d) schematics of the laser focus on the ground surface.

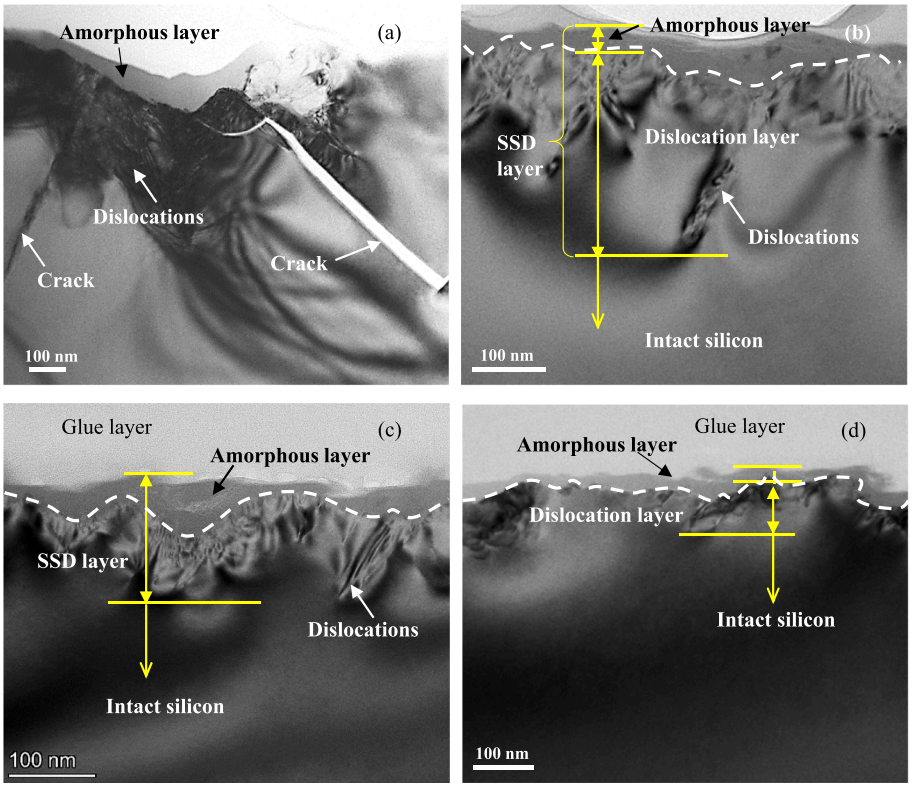

Fig. 3. TEM images of the SSD of the wafers ground by (a) the #600 wheel, (b) the #3,000 wheel, (c) the #5,000 wheel, and (d) the #20,000 wheel, respectively.

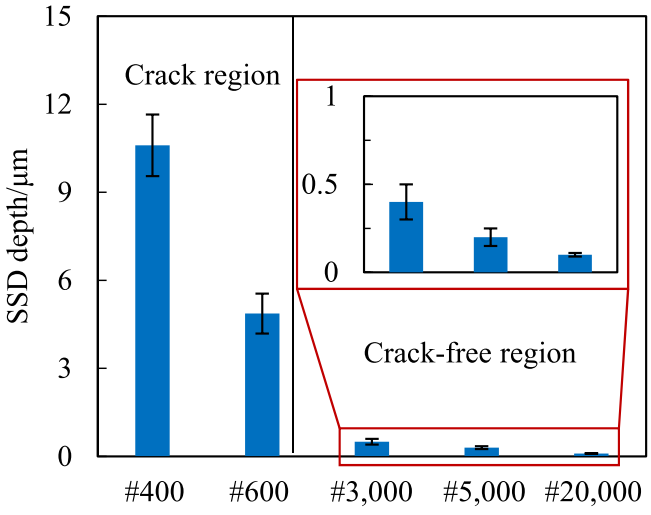

Fig. 4. SSD depth distribution in the ground wafers.

variations of the PLS detection results with surface roughness and SSD depth of the chosen wafer samples. As shown in Fig. 5, the SSD depths of the two samples were nearly the same, around 5.5 μm, while the surface roughness of the two samples presented a difference of around 30%. In this case, the detected laser power demonstrated little difference, as shown in Fig. 7. As shown in Fig. 6, the SSD depths of the two samples were different, one being 11.3 μm, while the other being 5.5 μm. The surface roughness of the two samples presented almost no difference. In this case, the detected PLS laser power represents a notable dependence on the SSD depth, as shown in Fig. 7. Therefore, the main influence factor of the PLS detection in this study is the SSD depth, whereas the influence of the surface roughness on the detection of SSD can be neglected.

The normalized PLS detection signals of the wafers are shown in Fig. 8. The wafer ground by the #400 wheel presented the strongest signal. The fluctuation of the PLS signal was also the largest, which resulted from the discontinuous distribution of SSD. The protrusion height of the abrasives on the wheel was not uniform, which lead to different depths of cut by the individual abrasives during grinding. Correspondingly, the SSD depth was not constant due to the non-uniform depth of cut. A large SSD depth results in a strong PLS detection signal. As the mesh number of the abrasives in the wheel increased, the SSD depth signal decreased, correspondingly, the normalized PLS signal decreased. Meanwhile, the deviation of SSD was also reduced with increasing the mesh number of the abrasives, as shown in Fig. 3. Therefore, the fluctuation of the normalized PLS detection signal also decreased. It was found that the PLS detection signal was sensitive to SSD depth. The minimum detectable SSD depth was about 0.1 μm.

There is the attenuation in the PLS detection signal with an increase in scanning distance, as shown in Fig. 8. It shows that the attenuation trends are the same among the PLS signals. This attenuation in the PLS signal was mainly caused by the mechanical installation error. The translation motion was not perfectly perpendicular to the laser beam. It had a small angle to the direction that is perpendicular to the laser beam. The distance between the wafer ground surface and lens increased during the translation motion, which enlarges the focused laser spot size on the wafer surface. Therefore, the radiation laser power density was decreased and therefore, the corresponding PLS detection signal attenuated with the scanning distance.

The PLS detection signal increases with the SSD depth. The relationship between the normalized PLS detection signal and SSD depth was fitted, as shown in Fig. 9. It shows that the normalized PLS detection signal y has a power-law relationship with the SSD depth δ, i.e., $y = 1.86\delta^{0.25}$. The coefficient of the determination of the relationship is $R^2 = 0.94$. The relationship is easy to use for quantifying SSD depth.

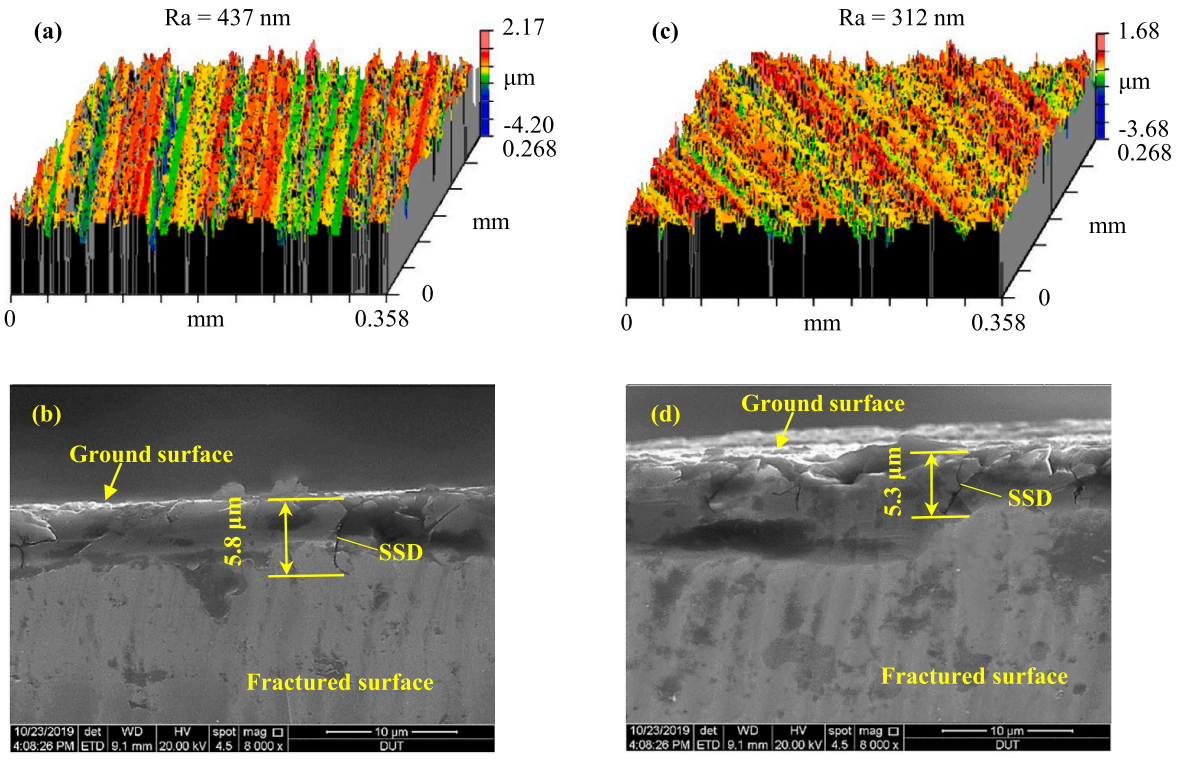

Fig. 5. The surface and subsurface morphologies of the wafer samples with the same SSD depth but different surface roughness. (a) and (b) the sample ground by the #600 wheel without the spark-out process. (c) and (d) the sample ground by the #600 wheel with the spark-out process.

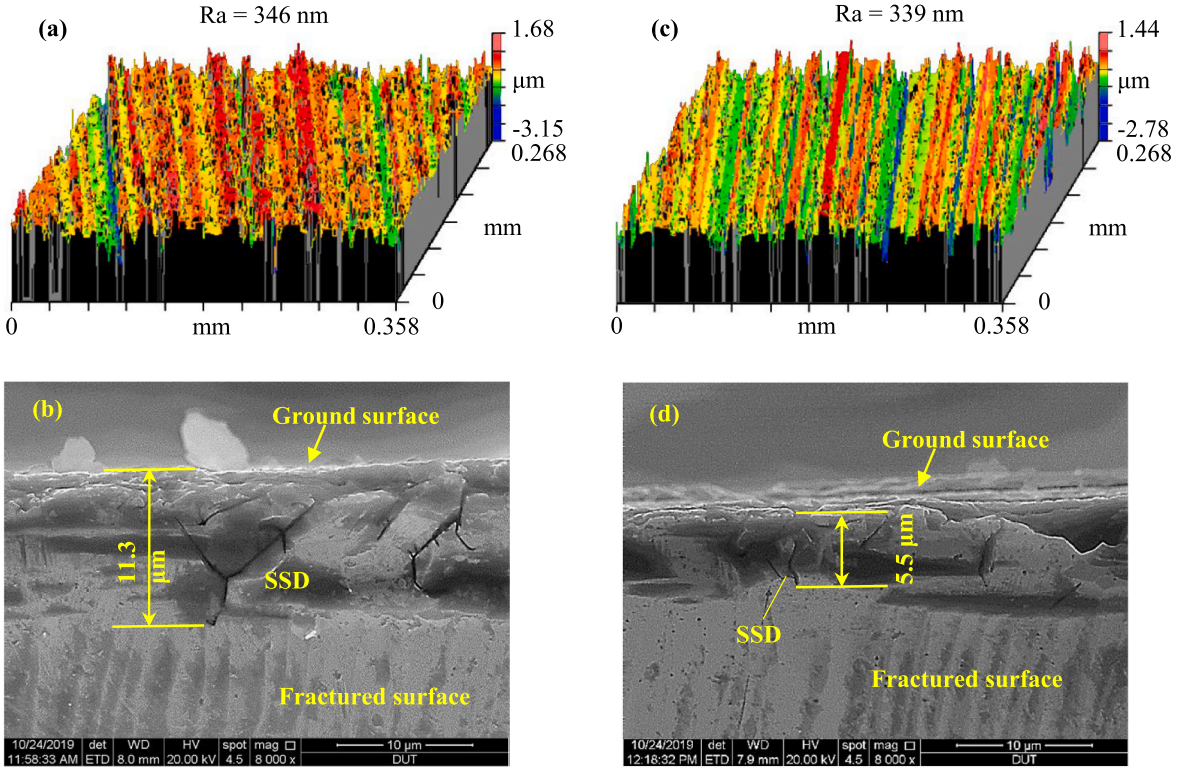

Fig. 6. The surface and subsurface morphologies of the samples with the same SSD depth but different surface roughness. (a) and (b) the sample ground by the wafer ground by the #400 wheel with the spark-out process. (c) and (d) the sample ground by the wafer ground by the #600 wheel without the spark-out process.

4. Discussion

The residual stress-induced photoelasticity is dependent on the difference between the two principal stresses and the angle of the polarization of the incident laser beam to the principal stress direction. In this study, the effects of residual stress were expected to be suppressed as

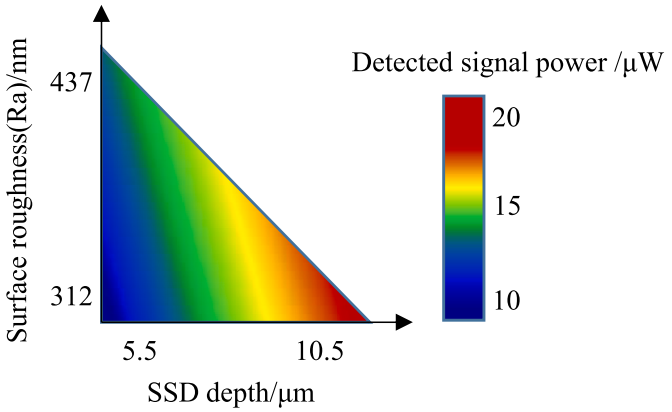

Fig. 7. Dependence of the detected PLS laser signal power on the surface roughness and SSD depth.

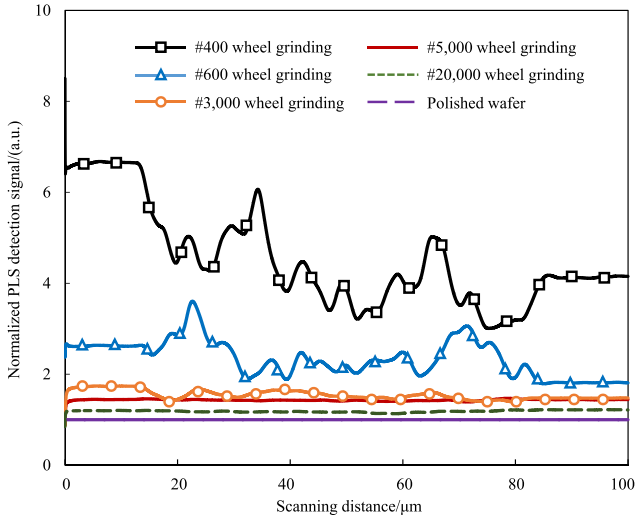

Fig. 8. Variations of the normalized PLS detection signals of the ground wafers.

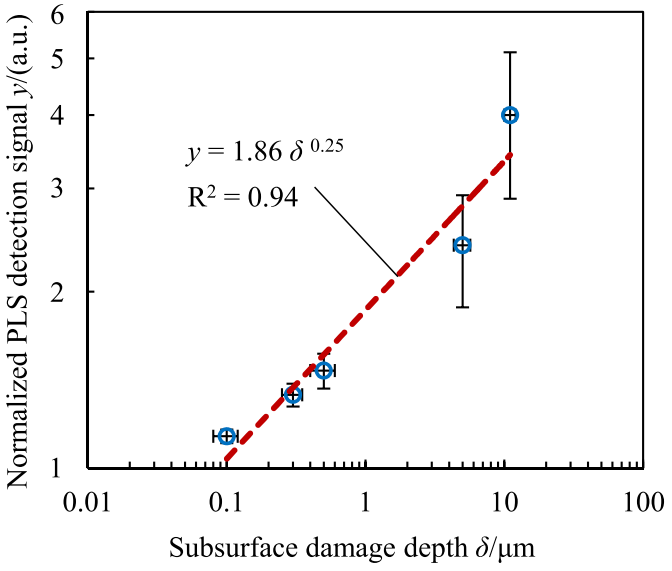

Fig. 9. Relationship between the normalized PLS detection signal and SSD depth.

much as possible based on the method proposed by Yin et al. [29]. In a large area, the directions of the principal stresses were determined by surface grinding marks [13,33]. However, the light was focused within a micro-region in which the residual stress distribution is extremely uneven. Zhang et al. [34] found that the variation of residual stress could be over 200 MPa in a few μm on the ground silicon surface and closed to 2 GPa in a few μm into the surface. Chen et al. [35] claimed that the variation of the residual stress even exceeded 2 GPa in a few nanometers into the surface. Therefore, it is difficult to eliminate the effects of residual stress.

Both the #400 wheel grinding and #600 wheel grinding induce cracks into the wafers. The PLS detection mainly attributes to both the multi-scattering by the subsurface crack walls and residual stress-induced photoelasticity. For a wafer ground by the wheel with the mesh number larger than #3,000, SSD consists of dislocations and amorphization instead of cracks. Therefore, the PLS signals of the wafers ground by the #3,000, #5,000, and #20,000 wheels attribute to the residual stress-induced photoelasticity. Therefore, the wafers ground by the #400 wheel and the #600 wheel represent stronger PLS signals than the rest wafers.

The PLS signal distributions of the wafers ground by the #3,000, #5,000, and #20,000 wheels are analyzed as follows. According to the theory of photoelasticity, the residual stress-induced PLS signal can be calculated by Eq. (1) [29].

$$I_s = I_i \cdot \sin^2(2\theta) \cdot \sin(\varphi/2) \tag{1}$$

where I_s and I_i are the scattered light intensity, respectively; θ is the angle between the polarization plane of the incident light and the first principal stress; φ is the phase retardation, expressed as Eq. (2).

$$\varphi = 2\pi \cdot C \cdot d \cdot (\sigma_1 - \sigma_2)/\lambda \tag{2}$$

where C is the stress-optic coefficient of silicon. In this paper, C is chosen as 1.6×10^{-11} Pa^{-1} d represents the thickness of the stressed layer, which is dependent on the SSD depth δ. λ is the wavelength of the incident light, i.e., 914 nm σ_1 and σ_2 are the first and second principal stresses, respectively. The scanning distance by the PLS detection is 100 μm. The directions of the principal stresses can be averaged over the scanning distance. Therefore, the angle between the polarization plane of the incident light and the first principal stress can be regarded as the same in these wafers. The main difference in the PLS signal of these wafers should come from the difference in the phase retardation. Based on the previous studies [33–35], the difference between the two principal stresses varies from hundreds of MPa to several GPa. Based on Eq. (2), by substituting the values of the determined parameters, the phase retardation can be estimated. It is found that the phase retardation is mainly dependent on the thickness of the stressed layer d. Therefore, the residual stress-induced PLS signal is dependent on the SSD depth δ.

Although the depolarization mechanisms of the PLS detection in those wafers are different, the PLS signal is correlated with the SSD depth. The larger the SSD depth, the more light the depolarization. The relationship is obvious between the PLS signal and SSD depth, which is in favor of the quantitative evaluation of SSD depth by the PLS method.

The sensitivity of the PLS detection is determined as the derivation with respect to the SSD depth δ, as shown as Eq. (3).

$$Se = \frac{dy}{d\delta} = 0.465.\delta^{-0.25} \tag{3}$$

Based on Eq. (3), the sensitivity of the PLS detection of the ground wafers are 0.08, 0.14, 0.92, 1.55, 2.61 for the wafers ground by the #400, #600, #3,000, #5,000, and #20,000 wheels, respectively. It can be found that the sensitivity of the PLS detection increases with decreasing the SSD depth. Namely, the PLS detection is more sensitive to the SSD depth in a fine grinding wafer, which is greatly promising for detecting the SSD in the wafers by ultraprecision grinding. However, the subsurface condition of the wafer by ultrafine grinding is complicated.

The stress distribution and the contributions of the amorphization and dislocations to the PLS detection are still unclear. Therefore, the PLS detection of the specific damages requires further investigations in the future.

5. Conclusions

The silicon wafers were ground by different wheels, which resulted in SSD with their depth ranging from submicron to about 10 μm. The SSD depth of the wafers was detected by the PLS method. The main findings in this study are listed as follows.

(1) The influence of surface roughness can be neglected in the PLS detection. SSD depth is the main factor.
(2) The PLS detection signal is sensitive to SSD depth. The minimum detectable SSD depth by the constructed PLS system is 0.1 μm.
(3) The PLS detection signal monotonically increases with SSD depth in a power-law relationship.

Author statements

Jingfei Yin: Conceptualization; Funding acquisition; Investigation; Methodology; Writing - original draft. **Qian Bai:** Supervision; Writing - review & editing. **Bi Zhang:** Supervision; Project administration; Writing - review & editing.

Declaration of competing interest

The authors declare that they have no known competing financial interests or personal relationships that could have appeared to influence the work reported in this paper.

Acknowledgments

Funding to this study from the National Natural Science Foundation of China (Nos. 51575084 and 52105453) and the Project Funded by China Postdoctoral Science Foundation (Nos. 2020TQ0149 and 2021M691569) are gratefully acknowledged.

References

[1] N. Qaiser, S.M. Khan, M.M. Hussain, In-plane and out-of-plane structural response of spiral interconnects for highly stretchable electronics, J. Appl. Phys. 124 (3) (2018), 034905, https://doi.org/10.1063/1.5031176.
[2] A.C. Cavazos Sepulveda, M.S. Diaz Cordero, A.A.A. Carreño, J.M. Nassar, M. M. Hussain, Stretchable and foldable silicon-based electronics, Appl. Phys. Lett. 110 (13) (2017) 134103, https://doi.org/10.1063/1.4979545.
[3] W. Guo, S.K. Anantharajan, X. Zhang, H. Deng, A study on the damage layer removal of single-crystal silicon wafer after atmospheric-pressure plasma etching, J. Micro Nano-Manufacturing 8 (2) (2020), https://doi.org/10.1115/1.4046377.
[4] M. Ge, H. Zhu, C. Huang, A. Liu, W. Bi, Investigation on critical crack-free cutting depth for single crystal silicon slicing with fixed abrasive wire saw based on the scratching machining experiments, Mater. Sci. Semicond. Process. 74 (2018) 261–266, https://doi.org/10.1016/j.mssp.2017.10.027.
[5] J. Yin, Q. Bai, Y. Li, B. Zhang, Formation of subsurface cracks in silicon wafers by grinding, Nanotechnol. Precis. Eng. 1 (3) (2018) 172–179, https://doi.org/10.1016/j.npe.2018.09.003.
[6] X. Li, Y. Gao, P. Ge, L. Zhang, W. Bi, The effect of cut depth and distribution for abrasives on wafer surface morphology in diamond wire sawing of PV polycrystalline silicon, Mater. Sci. Semicond. Process. 91 (2019) 316–326, https://doi.org/10.1016/j.mssp.2018.12.004.
[7] Y. Gao, P. Ge, L. Zhang, W. Bi, Material removal and surface generation mechanisms in diamond wire sawing of silicon crystal, Mater. Sci. Semicond. Process. 103 (2019) 104642, https://doi.org/10.1016/j.mssp.2019.104642.
[8] J. Yin, Q. Bai, S. Goel, P. Zhou, B. Zhang, An analytical model to predict the depth of sub-surface damage for grinding of brittle materials, CIRP J. Manuf. Sci. Technol. 33 (2021) 454–464, https://doi.org/10.1016/j.cirpj.2021.03.019.
[9] Z. Zhang, P. Chen, F. Qin, T. An, H. Yu, Mechanical properties of silicon in subsurface damage layer from nano-grinding studied by atomistic simulation, AIP Adv. 8 (5) (2018), 055223, https://doi.org/10.1063/1.5021654.
[10] J. Yin, Q. Bai, B. Zhang, Methods for detection of subsurface damage: a review, Chin. J. Mech. Eng. 31 (1) (2018) 41, https://doi.org/10.1186/s10033-018-0229-2.
[11] A. Solhtalab, H. Adibi, A. Esmaeilzare, S.M. Rezaei, Cup wheel grinding-induced subsurface damage in optical glass BK7: an experimental, theoretical and numerical investigation, Precis. Eng. 57 (2019) 162–175, https://doi.org/10.1016/j.precisioneng.2019.04.003.
[12] H.N. Li, T.B. Yu, L.D. Zhu, W.S. Wang, Evaluation of grinding-induced subsurface damage in optical glass BK7, J. Mater. Process. Technol. 229 (2016) 785–794, https://doi.org/10.1016/j.jmatprotec.2015.11.003.
[13] P. Zhou, S. Xu, Z. Wang, Y. Yan, R. Kang, D. Guo, A load identification method for the grinding damage induced stress (GDIS) distribution in silicon wafers, Int. J. Mach. Tool Manufact. 107 (2016) 1–7, https://doi.org/10.1016/j.ijmachtools.2016.04.010.
[14] C. Ma, W. Arnold, Nanoscale ultrasonic subsurface imaging with atomic force microscopy, J. Appl. Phys. 128 (18) (2020) 180901, https://doi.org/10.1063/5.0019042.
[15] J. Attal, C.F. Quate, Investigation of some low ultrasonic absorption liquids, J. Acoust. Soc. Am. 59 (1) (1976) 69–73, https://doi.org/10.1121/1.380827.
[16] R.G. Maev, 6 - acoustic microscopy for materials characterization, in: G. Hübschen, I. Altpeter, R. Tschuncky, H.-G. Herrmann (Eds.), Materials Characterization Using Nondestructive Evaluation (NDE) Methods, Woodhead Publishing, 2016, pp. 161–175.
[17] A.A. Karabutov, N.B. Podymova, Study on the subsurface damage depth in machined silicon wafers by the laser-ultrasonic method, Case Stud. Nondestruct. Testing Eval. 1 (2014) 7–12, https://doi.org/10.1016/j.csndt.2014.03.002.
[18] C.W. Hardin, J. Qu, A.J. Shih, Fixed abrasive diamond wire saw slicing of single-crystal silicon carbide wafers, Mater. Manuf. Process. 19 (2) (2004) 355–367, https://doi.org/10.1081/AMP-120029960.
[19] P. Cloetens, M. Pateyron-Salomé, J.Y. Buffière, G. Peix, J. Baruchel, F. Peyrin, M. Schlenker, Observation of microstructure and damage in materials by phase sensitive radiography and tomography, J. Appl. Phys. 81 (9) (1997) 5878–5886, https://doi.org/10.1063/1.364374.
[20] A. Haapalinna, S. Nevas, D. Pähler, Rotational grinding of silicon wafers—sub-surface damage inspection, Mater. Sci. Eng., B 107 (3) (2004) 321–331, https://doi.org/10.1016/j.mseb.2003.12.008.
[21] M.D. Biasio, L. Neumaier, N. Vollert, E. Geier, M. Roesner, H. Ch, M. Kraft, Determination of stress in silicon wafers using Raman spectroscopy, in: Proc.SPIE, 2015, https://doi.org/10.1117/12.2176994.
[22] H.D. Geiler, H. Karge, M. Wagner, A. Ehlert, E. Daub, K. Messmann, Detection and analysis of crystal defects in silicon by scanning infrared depolarization and photoluminescence heterodyne techniques, Mater. Sci. Eng., B 91–92 (2002) 46–50, https://doi.org/10.1016/S0921-5107(01)00965-5.
[23] X. Wu, W. Gao, Y. He, H. Liu, Quantitative measurement of subsurface damage with self-referenced spectral domain optical coherence tomography, Opt. Mater. Express 7 (11) (2017) 3919–3933, https://doi.org/10.1364/OME.7.003919.
[24] J. Neauport, P. Cormont, P. Legros, C. Ambard, J. Destribats, Imaging subsurface damage of grinded fused silica optics by confocal fluorescence microscopy, Opt Express 17 (5) (2009) 3543–3554, https://doi.org/10.1364/OE.17.003543.
[25] C. Schinke, P. Christian Peest, J. Schmidt, R. Brendel, K. Bothe, M.R. Vogt, I. Kröger, S. Winter, A. Schirmacher, S. Lim, H.T. Nguyen, D. MacDonald, Uncertainty analysis for the coefficient of band-to-band absorption of crystalline silicon, AIP Adv. 5 (6) (2015), 067168, https://doi.org/10.1063/1.4923379.
[26] J. Wang, Y. Li, J. Han, Q. Xu, Y. Guo, Evaluating subsurface damage in optical glasses, J. Eur. Opt. Soc. Rapid Pub. 6 (2011).
[27] Z.M. Liao, S.J. Cohen, J.R. Taylor, Total Internal Reflection Microscopy (TIRM) as a Nondestructive Subsurface Damage Assessment Tool, Proc.SPIE, 1995, https://doi.org/10.1117/12.213733.
[28] W.K. Lu, J.G. Sun, Z.J. Pei, Subsurface damage measurement in silicon wafers with cross-polarisation confocal microscopy, Int. J. Nanomanufacturing 1 (2) (2006) 272–282, https://doi.org/10.1504/IJNM.2006.012198.
[29] J. Yin, Q. Bai, B. Zhang, Subsurface damage detection on ground silicon wafers using polarized laser scattering, J. Manuf. Sci. Eng. 141 (10) (2019), https://doi.org/10.1115/1.4044417.
[30] J. Yin, Q. Bai, H. Haitjema, B. Zhang, Two-dimensional detection of subsurface damage in silicon wafers with polarized laser scattering, J. Mater. Process. Technol. 284 (2020) 116746, https://doi.org/10.1016/j.jmatprotec.2020.116746.
[31] Z.J. Pei, A. Strasbaugh, Fine grinding of silicon wafers, Int. J. Mach. Tool Manufact. 41 (5) (2001) 659–672, https://doi.org/10.1016/S0890-6955(00)00101-2.
[32] M. Trost, T. Herffurth, D. Schmitz, S. Schröder, A. Duparré, A. Tünnermann, Evaluation of subsurface damage by light scattering techniques, Appl. Opt. 52 (26) (2013) 6579–6588, https://doi.org/10.1364/AO.52.006579.
[33] P. Zhou, Y. Yan, N. Huang, Z. Wang, R. Kang, D. Guo, Residual stress distribution in silicon wafers machined by rotational grinding, J. Manuf. Sci. Eng. 139 (8) (2017), https://doi.org/10.1115/1.4036125.
[34] Y. Zhang, D. Wang, W. Gao, R. Kang, Residual stress analysis on silicon wafer surface layers induced by ultra-precision grinding, Rare Met. 30 (3) (2011) 278–281, https://doi.org/10.1007/s12598-011-0383-5.
[35] P. Chen, Z. Zhang, T. An, H. Yu, F. Qin, Generation and distribution of residual stress during nano-grinding of monocrystalline silicon, Jpn. J. Appl. Phys. 57 (12) (2018) 121302, https://doi.org/10.7567/jjap.57.121302.